



Wall Shear Stress Generated by Aqueous Flowing Foam

Rogelio Chovet, Fethi Aloui, Laurent Keirsbulck

► To cite this version:

Rogelio Chovet, Fethi Aloui, Laurent Keirsbulck. Wall Shear Stress Generated by Aqueous Flowing Foam. ASME/JSME/KSME 2015 Joint Fluids Engineering Conference, Jul 2015, Séoul, South Korea. 10.1115/AJKFluids2015-14039 . hal-03433925

HAL Id: hal-03433925

<https://uphf.hal.science/hal-03433925>

Submitted on 8 Jul 2022

HAL is a multi-disciplinary open access archive for the deposit and dissemination of scientific research documents, whether they are published or not. The documents may come from teaching and research institutions in France or abroad, or from public or private research centers.

L'archive ouverte pluridisciplinaire **HAL**, est destinée au dépôt et à la diffusion de documents scientifiques de niveau recherche, publiés ou non, émanant des établissements d'enseignement et de recherche français ou étrangers, des laboratoires publics ou privés.



Distributed under a Creative Commons Attribution - NonCommercial 4.0 International License

WALL SHEAR STRESS GENERATED BY AQUEOUS FLOWING FOAM

Rogelio Chovet

rogelio.chovet@univ-valenciennes.fr

Fethi Aloui *

* Corresponding author:

fethi.aloui@univ-valenciennes.fr

Laurent Keirsbulck

laurent.keirsbulck@univ-valenciennes.fr

LAMIH UMR CNRS 8201, University of Valenciennes (UVHC)
Department of Mechanics, Campus Le Mont Houy
59313 Valenciennes Cedex 9 – France

ABSTRACT

Aqueous foam flow over horizontal channels present significant pressure losses originated by the wall shear stress. Understanding this phenomenon is of paramount importance for the oil, food and cosmetic industries. In this study, we validate the use of the innovative polarographic method, used to measure the wall shear stress. It measures an oxy-reduction reaction controlled by the convection and diffusion phenomenon. The most reliable way of obtaining the wall shear stress is through the pressure losses. They allow obtaining the pressure gradient along the length of the channel, which can be related to an averaged wall shear stress. These measurement techniques were applied over a horizontal foam flow enclosed in a square duct of section 21 x 21 mm²; with a velocity of 2, 4 and 6 cm/s; and a void fraction of 70%. Results validate the use of the polarographic method to obtain the wall shear stress produced by foam flow inside a channel.

NOMENCLATURE

Roman letters

A	Probe surface
c_{∞}	Concentration at the flow core
CN	Cyanide
d_h	Hydraulic diameter
d_s	Probe diameter
D	Diffusion coefficient
e^-	Electron involved in chemical reaction
\vec{e}_x	Unit vector of the x axis
F	Faraday number
Fe	Iron
I	Polarographic current
L	Channel's length
P	Pressure
Q_g	Gas flow
Q_l	Liquid flow

Q_t	Total flow = $Q_t = Q_g + Q_l$
Sh	Sherwood number
So	Velocity Gradient
u	Axial velocity component
\vec{u}	Velocity vector
x, y, z	Cartesian coordinates
z_e	Electron number

Greek letters

β	Void fraction
Δ	Difference operator
μ_l	Liquid's dynamic viscosity
σ	Dimensionless frequency
τ	Wall shear stress
$\bar{\tau}$	Mean wall shear stress
τ_p	Polarographic wall shear stress
ω	Real pulsations

Abbreviation

PIV	Particle Image Velocimetry
-----	----------------------------

INTRODUCTION

What are the rheological properties of “foam”? Different scientists, coming most of them with similar answers, have discussed this item. The main objective of this experimental work has to do with this question; we approach it by studying the influence foam flow has over the walls of a channel, exerting a shear stress and generating pressure losses. Foams form by trapping pockets of gas in a liquid or solid. In most of them, the volume of gas is larger than the liquid one, which forms thin films separating it from the gas.

Foam has unusual rheology properties: they present low densities and an important interfacial surface. They are mainly composed of gas, but under low applied stress, it behaves as a solid; hence shaving foams adhere to the shaver's face, the weak

force of gravity being incapable of letting it flow. This results from an elastic shear modulus, as occurs in isotropic solid materials. They can also behave as an elastic solid or a plastic one. Beyond a certain yield stress, foam flows as topological changes are promoted indefinitely. This is the second most important parameter characterizing its rheological properties.

Foam flow has become a major study subject for industries around the world. In traditional “Secondary Recovery of Hydrocarbons”, for example, foam is injected in the reservoirs to displace and recovery some of the residual oil in-situ. It is indispensable to better understand its rheological properties, especially the knowledge of the wall shear stress and pressure losses it generates inside close channels. Most of the studies carried out focus on the geometry and topology of stationary foams and not on the flow itself, due to its complexity [1,2].

Previous works tried to set a rheological model for foam flow, taking into account the pressure losses along a conduct. Others added an innovative measurement method to combine the pressure losses and the wall shear stress. But at the end, they could not collect enough data to draw a model. The major problem is that a foam flow is influenced by an enormous quantity of parameters. Looking at the high interest shown for foam flow along the industries, it is indispensable to achieve the capacity to understand and evaluate several variables concerning the hydraulic behavior: pressure losses, velocity distribution and wall shear stress [3,4,5,6].

This experimental work combined all the concerning variables to validate the use of the polarographic technique over flowing foams to obtain a reliable value of the wall shear stress. Through this research, we will like to understand the behavior of foam flow: its physics, stability and hydrodynamics. The objective at the end is to establish or validate rheological modes that will allow predicting the behavior or aqueous foam flow.

MATERIAL AND METHODS

Experimental device

The experimental facility was designed to handle the different requirements of foam flow. It has a geometry capable of making studies for horizontal foam flows. It presents plane walls making it suitable for the experimental measurements undertaken. Thus, the plane walls allowed the easy placement of polarographic probes along its surface. They are required in the Particle Imaging Velocimetry.

A schematic representation of the experimental facility appears in Figure 1. It includes two adjacent ducts; the test section covers a close liquid circuit and an open gas one. Inside the second duct is where the polarographic method calibration takes place. The recuperation tank recovers the liquid through the drainage of the foam, while the charge one assures a constant liquid pressure inside the foam generators, avoiding the flow

fluctuations created by the centrifugal pump. The foam is created injecting pressured air, through a permeable media inside cylindrical containers filled with liquid (water with surfactant and polarographic solution at $20 \pm 1^\circ\text{C}$).

Foams may be classified as dry or wet accordingly to its liquid content, which may be represented by the gas volume fraction. Engineers call this one “foam quality”, it can be represented by the equation:

$$\beta = \frac{Q_g}{Q_l + Q_g} \dots\dots\dots(1)$$

where Q_g is the gas flow and Q_l the liquid flow.

A way to evaluate horizontal foam flow inside a channel is through its global velocity for a foam quality of 70% three different regimes can be observed. They result from the interpolation of the velocity and, measured at the ducts wall, over a straight section. The three different flow regimes are [3]:

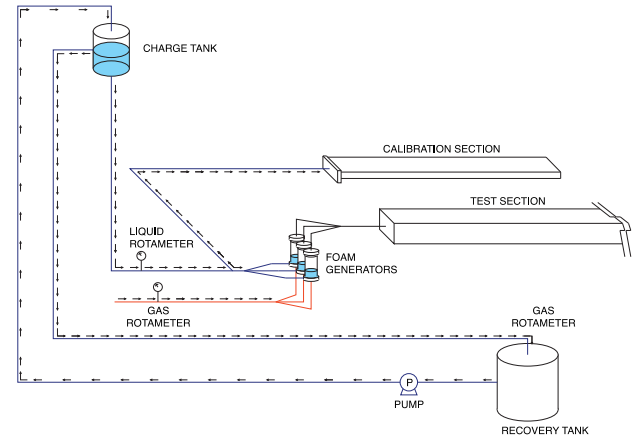


FIGURE 1. SCHEMATIC REPRESENTATION OF THE EXPERIMENTAL FACILITY

One-dimensional flow: Inside this regime, for slow velocities, the flow behaves as a whole. It moves like a block or a piston and its velocity vectors have one uniform axial component in the axial flow direction.

$$\vec{u} = u \cdot \vec{e}_x = cte \cdot \vec{e}_x \dots\dots\dots(2)$$

Two-dimensional flow: It is obtained when the established flow velocity vectors depend only of the y coordinate.

$$\vec{u} = u(y) \cdot \vec{e}_x \dots\dots\dots(3)$$

Three-dimensional flow: The axial flow velocity component depends on the z and y coordinates.

$$\vec{u} = u(y, z) \cdot \vec{e}_x \dots\dots\dots(4)$$

The presence of three generators, parallels and independent, allow us to modify the foam flow and bulk velocity (one generator for 2 cm/s, two generators for 4 cm/s and three generators for 6 cm/s) without altering the foam structure. The

foam quality is established at 70%, which represents an aqueous foam flow. The liquid and gas flow were measured with several rotameters (Brooks).

The test duct has a length of approximately 3.2 m and is made of Plexiglas with a 21 x 21 mm² square section. The middle of the test section is composed by a measurement part, located 1.3 m downstream from the foam generators. At this point three measurement blocks were used to determine the wall shear stress over the top, bottom and lateral wall of the channel (Figure 2). Each block contains 11 polarographic probes and can be moved from the test section to the auxiliary channel.

The probes diameter will affect the reading; the smaller the electrode better will be the phenomenon acquisition and response. This point is confirmed by the relationship [7]:

$$\sigma = \omega \left(\frac{d_s^2}{D S_0^2} \right)^{1/3} \dots\dots\dots (5)$$

Where σ is the dimensionless frequency, $\omega = 2\pi f$ the real pulsations, d_s the probes diameter, D the diffusion coefficient, and S_0 the velocity gradient.

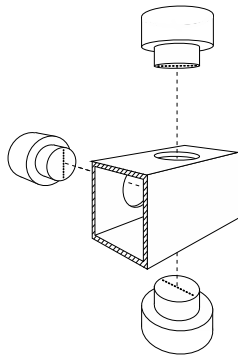


FIGURE 2. SETTING ARRANGEMENT OF THE THREE POLAROGRAPHIC BLOCKS

The probes in the experiment had a diameter around $d_s = 0.25 \text{ mm}$, equivalent to a theoretical rectangular probe with a length of $l = 0.82 d_s$ [7]. They were spaced 2 mm from each other, and aligned perpendicularly to the flow (Figure 3).

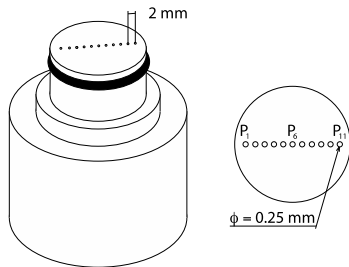


FIGURE 3. POLAROGRAPHIC PROBES

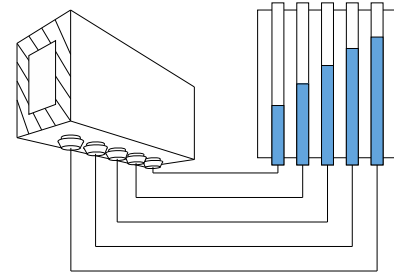


FIGURE 4. DIAGRAM OF THE PRESSURE LOSSES ARRANGEMENT

Measurement techniques

The static pressure along the test section is measured by pressure outlets located at the bottom of the channel, at the middle vertical plane. These pressure outlets are attached through silicon hoses, to a series of manifold tubes placed over a scaled plate (Figure 4). The misreading of the manifold pipes is estimated at a maximum 1 mm water column. There are 8 pressure outlets along the channel length.

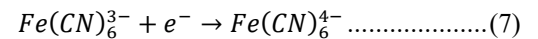
The pressure value at each water column height is calculated by the Bernoulli equation:

$$P = P_a + \Delta z \rho g + v^2 \rho \dots\dots\dots (6)$$

Where P_a is the atmospheric pressure, Δz the height difference between the water column height measured at the pressure outlet and the one measured for the atmospheric pressure, ρ the liquid density, g the gravity acceleration, and v is the foam velocity.

The Particle Imaging Velocimetry (PIV) is a non-intrusive method capable of measuring the displacement of particle in a plane. It is done by the comparison between two instantaneous position fields of particles in the flow. It is possible to calculate mean velocity fields and profiles by this particle displacement. In foams, the gas/liquid interphases are darker than the rest of the flow, and the bubbles contour assigns the whole flow movement. Therefore, the use of particles is not necessary to track the flow. The close packing of the bubbles keeps them together along the channels length; avoiding the error that bubbles displacement might generate. The measurements were made over the channel lateral wall. Due to the opacity of the foam, and the reflections over the bubbles it is impossible to see through it; and obtain the internal velocity fields. Nevertheless, the main focus is the wall/foam interactions.

The wall shear stress is experimentally determined using circular electrode surfaces. For the polarographic method the ferri-ferrocyanide couple was selected. This one is very suitable for this study, because of its power and its small sensitivity to the light. The cathode reduction obeys the equation:



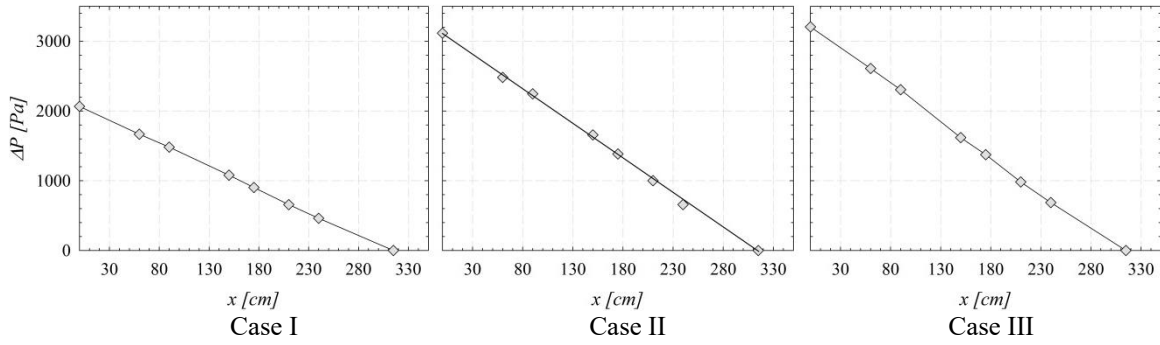


FIGURE 5. STATIC PRESSURE LOSSES ALONG THE SQUARE CHANNEL FOR CASES I, II AND III

The couple exchanges one electron. The chemical reaction is fast enough to not affect the electrodes surfaces. The active ions concentration is constant through the experiment. The limiting diffusion current was converted to voltage using a system electrometer.

In order to restrain the amount of electrolysis reagent, the ferricyanide concentration was 10 mol/m^3 . This amount allows measuring the intensity of the diffusion current (micro-amperes). The ferrocyanide concentration is 15 mol/m^3 , so the reaction over the anode is not a limitation to the current circulation. The concentration of potassium sulfate, 175 mol/m^3 , reduces the solution resistivity, neutralizing the ion migration due to the potential field created between the cathode and the anode.

RESULTS AND DISCUSSIONS

The experimental results obtained from the pressure outlet, the PIV and the polarographic method are presented in the form of pressure losses, velocity profiles and Sherwood numbers respectively.

Pressure Losses

The pressure losses inside the channel are represented in Figure 5. In all the cases the static pressure varies linearly all through the channel.

For the three cases a constant pressure gradient occurs. The pressure gradient results validate the analysis that faster foams generate bigger pressure losses. They show that the change in the linearity can be a result of the change in the foam velocity. Therefore, a deeper study was carried in order to understand the real causes of this behavior, specially focused in the wall shear stress.

Velocity Profiles

Indicated in previous works [3,8,6], the foam flowing through channels may be studied under three different regimes, as a function of the axial velocity. This property may be measured by the PIV technique. The axial velocity profiles for all three cases are represented as averaged velocity values, taken over 500 images (Figure 6).

We see an influence of the bottom liquid slip-layer over the profile. As the velocity increases the flow of the underlying liquid film does too. Therefore cases II and III, present a higher velocity near the bottom of the channel. Case I has a uniform axial velocity along the whole section (one-dimensional regime). The foam flow, for case II, is partially sheared at the bottom of the channel. Therefore, the axial velocity is not uniform and the flow becomes a two-dimensional regime. Finally for the last case, the foam flow will be completely sheared and its axial velocity also is displaced on the z coordinate.

Polarographic signals

The instantaneous polarographic signals are shown in Figure 7 to Figure 9. They were obtained at the middle of the test section; over three of the four walls: bottom, one lateral and top; for the three cases. These results represent the evolution of the Sherwood number over one second. This dimensionless number is linked to the probes diameter $-d_s-$ and the measured current $-I-$ through the following relationship:

$$Sh = \frac{I}{z_e F A c_\infty D} d_s \dots\dots\dots(8)$$

Where z_e is the electron number involved, F is the Faraday number, c_∞ is the concentration at the flow core, D is the diffusion coefficient and $A = \frac{\pi d_s^2}{4}$ is the probe's surface.

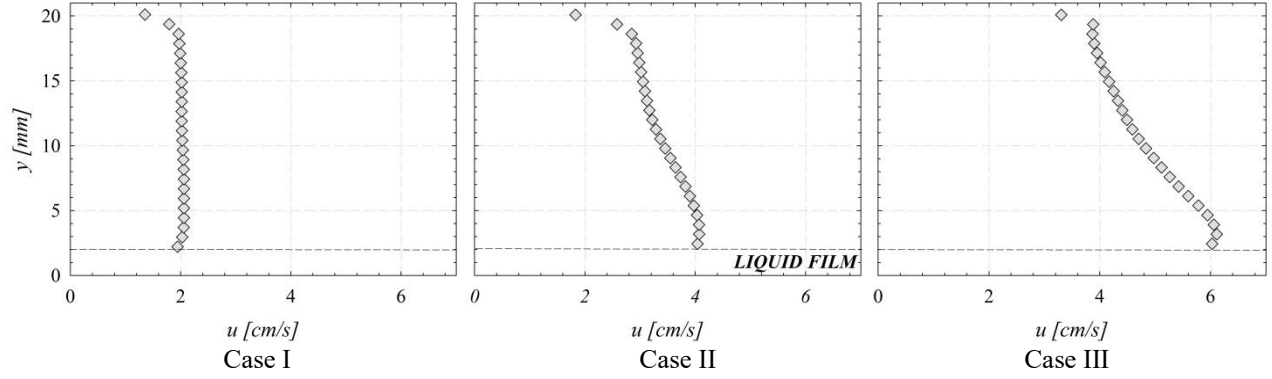


FIGURE 6. AVERAGE VELOCITY PROFILES AT THE LATERAL WALL FOR CASES I, II AND III

We can see that the signal fluctuations are a result of the bubbles passage over the electrode. Due to the gravitational foam flows are submitted, water tends to the bottom of the channel [9]. Therefore the probes closer to this part of the channel present less Sherwood fluctuations than the ones at the top. Here the liquid film thickness is smaller and the bubbles influence is important.

When comparing the Sherwood fluctuations for the three foam velocities it should be noted how the mean value of the Sherwood number increases with the velocity. The Sherwood number's fluctuation seems to be related somewhat to the foam velocity. The number of fluctuations per second is directly related to the number of bubbles passing by the probe. There is a resemblance in the behavior of the fluctuations between all three cases: at the bottom there are no fluctuations; at the top the fluctuations present the same form and at over the lateral wall a similar evolution from the upper part of the channel to the lowest one.

Wall shear stress

One notable aspect of the foam flow is its capacity to generate wall shear stress values 2000 times bigger than the water under the same regime. There are many ways to measure the wall shear stress of a fluid inside a channel. It depends of the velocity gradient inside the boundary layer and the pressure losses along a characteristic length. The pressure outlets located along the channel allow obtaining an accurate value of the pressure losses generated by the wall shear stress, and validating the polarographic method.

The wall shear stress is defined as:

$$\tau = \mu_l \frac{\delta u}{\delta y} \dots \dots \dots (9)$$

Where μ_l is the liquid's dynamic viscosity and $\frac{\delta u}{\delta y}$ the velocity gradient.

Foam flow presents complex properties that difficult defining the wall shear stress and the velocity gradient (opacity, reflections, small scales, etc.). We have followed two ways to

obtain the mean wall shear stress over the channel's square section.

From the polarographic signals, we can deduct the mean wall shear stress values along the length of the channel's walls, through the limit diffusion current [10]:

$$\tau_p = \frac{\mu_l}{(0.633 z_e F c_\infty)^3 D^2 d_s^5} I^3 \dots \dots \dots (9)$$

It has been shown for a polarographic probe of diameter, d_s , the mean value of the Sherwood number, \overline{Sh} , the characteristics of the liquid, which are the dynamic viscosity, μ_l , and the diffusion coefficient, D , the mean wall shear stress value, τ_p , can be obtained through:

$$\tau_p = \frac{\pi^3 \mu_l D}{8.95 d_s^2} Sh^3 \dots \dots \dots (10)$$

Where $\frac{\Delta p}{L}$ is the pressure gradient and $d_h = 21 \text{ mm}$ the hydraulic diameter.

These values were compared with the wall shear stress obtained through the polarographic method, to validate the measurement technique. For the polarographic method the mean wall shear stress along the channel's surface was calculated through the following equation.

$$\bar{\tau} = \frac{1}{4n} [\sum_i^n \tau_{bottom_i} + 2 \sum_i^n \tau_{lateral_i} + \sum_i^n \tau_{top_i}] \dots \dots (11)$$

The mean wall shear stress values obtained with the pressure losses and the polarographic signals are shown in Figure 10 for all cases.

The representation of the mean wall shear stress along the channel's surface; obtained with two different approaches (pressure losses and Sherwood number signal), allows us to validate the use of the polarographic method, for certain shears.

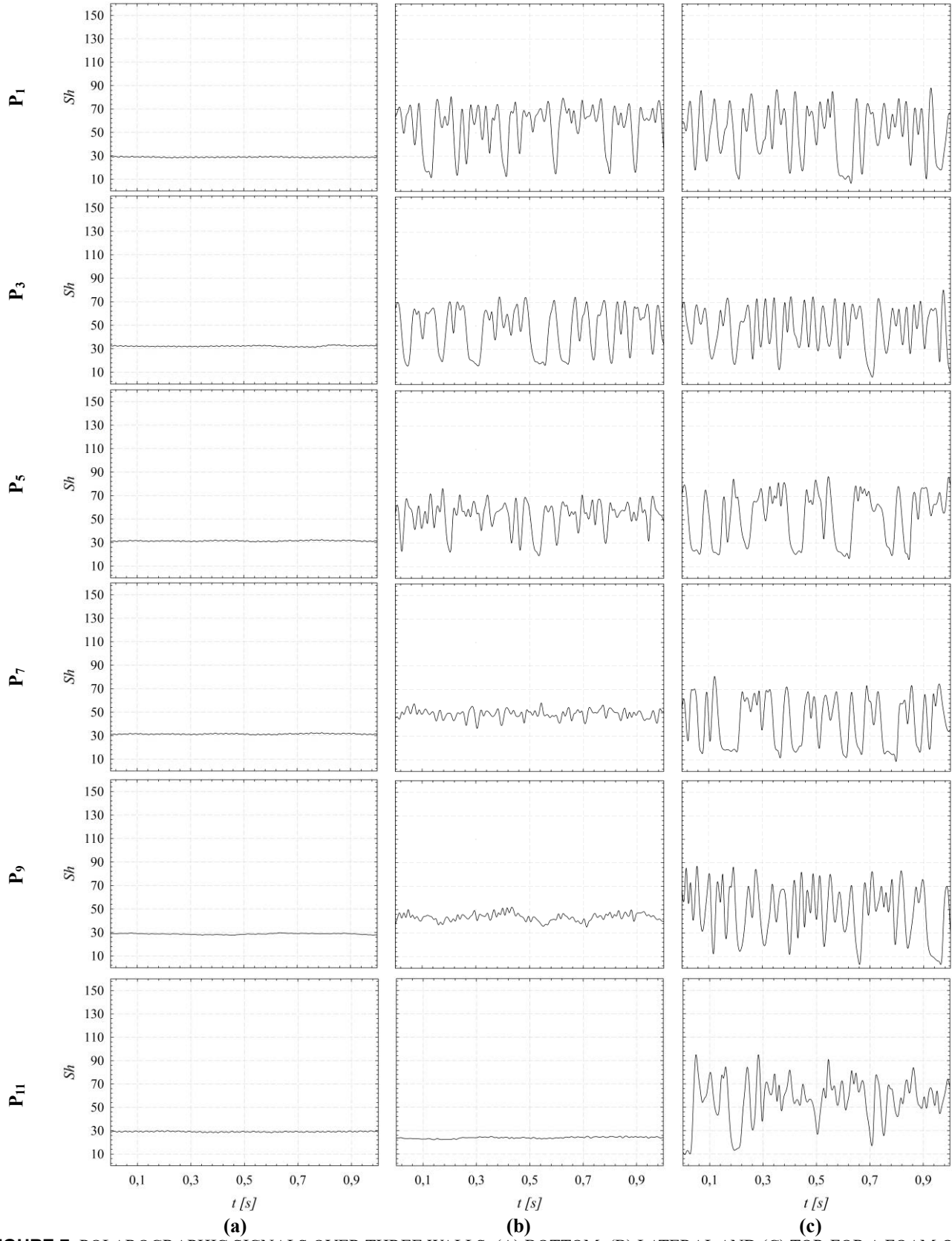


FIGURE 7. POLAROGRAPHIC SIGNALS OVER THREE WALLS: (A) BOTTOM, (B) LATERAL AND (C) TOP, FOR A FOAM QUALITY OF 70% AT 2 CM/S.

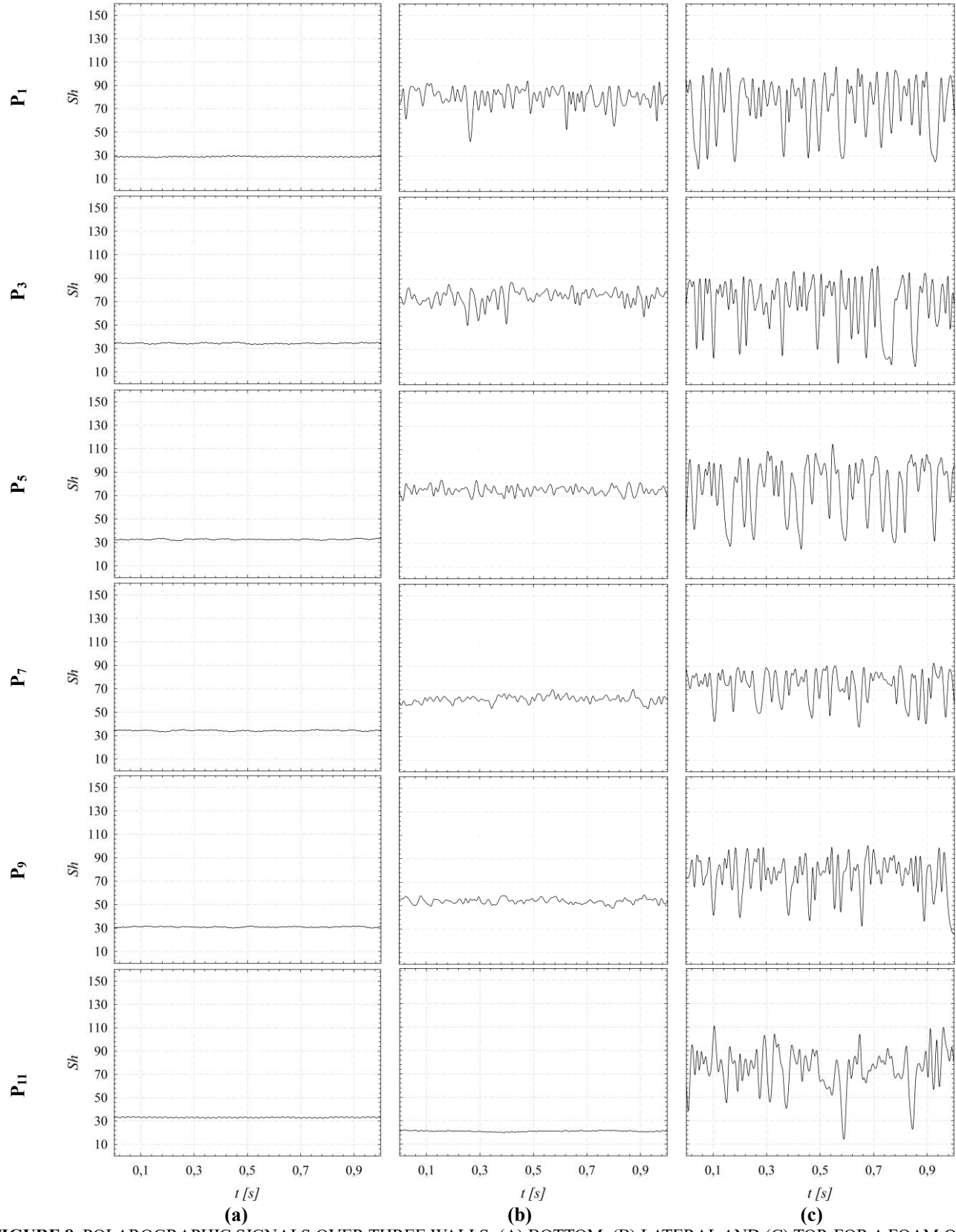


FIGURE 8. POLAROGRAPHIC SIGNALS OVER THREE WALLS: (A) BOTTOM, (B) LATERAL AND (C) TOP, FOR A FOAM QUALITY OF 70% AT 2 CM/S

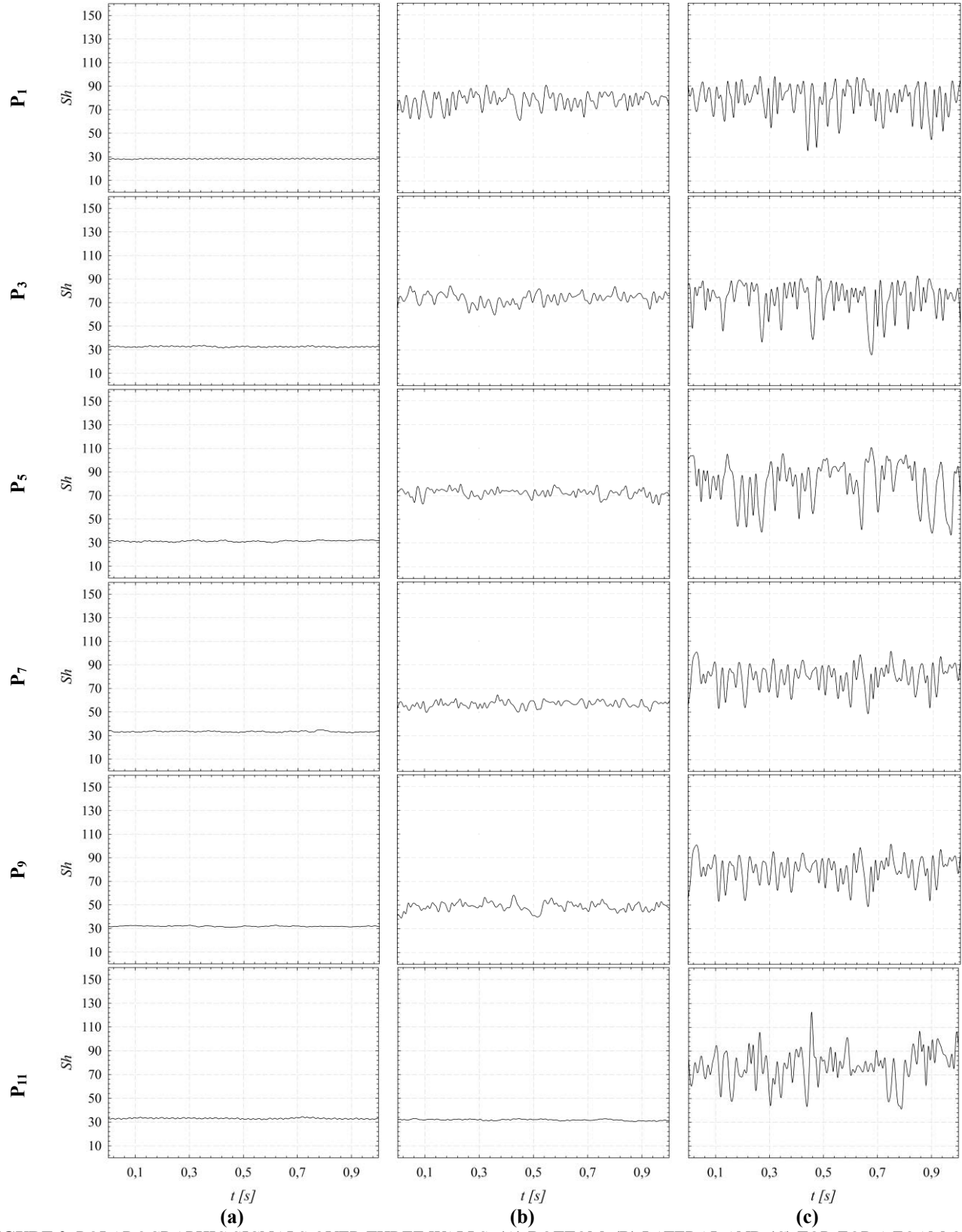


FIGURE 9. POLAROGRAPHIC SIGNALS OVER THREE WALLS: (A) BOTTOM, (B) LATERAL AND (C) TOP, FOR A FOAM QUALITY OF 70% AT 6 CM/S

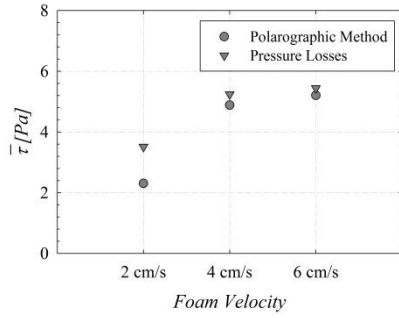


FIGURE 10. MEAN WALL SHEAR STRESS ALONG THE CHANNELS SURFACE FOR ALL THREE CASES

To better understand the behavior of our mean shear stress values we refer to Figure 11. It was developed by Tisné [11], which relates numerically the wall shear stress, the limit diffusion current and the liquid film thickness.

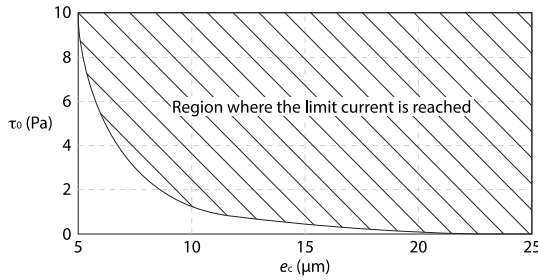


FIGURE 11. CURVE LIMITING THE REGION WHERE THE POLAROGRAPHIC SIGNAL DOES NOT DEPEND ON THE LIQUID FILM THICKNESS OR THE WALL SHEAR STRESS

All cases present similar liquid film thicknesses [9] but different wall shear stresses. Slower foams are more susceptible to fall inside the region where the limit diffusion current is not reached, and therefore not be able to measure the velocity gradient through the polarographic method. As the foam moves faster the threshold between the two regions diminishes and the limit diffusion current will be reached most of the time. This phenomenon can be seen over the mean shear stress comparison; as the foam velocity increases, the polarographic values resemble more the pressure losses ones, which are the most credible. The largest gap between the polarographic method and the pressure losses is of 43% for a foam velocity of 2cm/s, and wall shear stress values around 2 and 4 Pa fluctuating between the two regions, making less accurate the velocity gradient calculation. For a velocity of 6 cm/s the deviation reduces to 10%, the wall shear stress tends to 5.5 Pa, and the limit diffusion current is reached most of the time.

CONCLUSIONS

In this study the measurements of the static pressure, the velocity profile and the wall shear stress allowed us to understand the hydrodynamic behavior of foam flowing through a straight

channel for three different velocities. From pressure outlets located all along the channel's length, we defined the pressure losses, which are related to the foam velocity. Faster foams generate higher pressure gradients. Using the Particle Imaging Velocimetry (PIV) we were able to determinate the local axial velocity of the foam and identified the three regimes of foam flowing in horizontal square channels. Finally the polarographic method was verified. Polarographic signals were acquired for all cases. From these currents we were able to calculate the velocity gradient. To evaluate the use of the polarographic method, the wall shear stress thereof obtained was compared against the one calculated through the pressure losses. These results, validated the use of the polarographic method in the case of foams that present velocities over 6cm/s, they generate higher wall shear stresses and are not dependent on the thickness of the liquid film to reach a limit diffusion current. Further studies should analyze the influence of the void fraction over the wall shear stress generated and see if the polarographic method is still valid. Polarographic probes should be located over different flow disruption devices in order to quantify the wall shear stress exerted over these ones. Lastly a study of the liquid slip layer located between the foam and the walls should be done. These films are the one in direct contact with the channel and generate the important wall shear stresses seen in this study.

ACKNOWLEDGMENTS

This work was supported by the laboratory LAMIH CNRS UMR 8201 (University of Valenciennes), the laboratory LESTE (ENIM, Monastir, Tunisia) and the European Commission within the International Research Staff Exchange Scheme (IRSES) in the 7th Framework Programme FP7/2014-2017/ under REA grant agreement n°612230. These supports are gratefully acknowledged.

REFERENCES

- [1] D. Weaire and S. Hutzler, *The Physics of Foams*. Dublin: Oxford, 1999.
- [2] P. Stevenson, *Foam Engineering: Fundamentals and Applications*. Auckland, New Zealand: John Wiley & Sons, 2012.
- [3] E. Blondin and L. Doublier, "Particle Imaging Velocimetry of a wet aqueous foam with and underlying liquid film", *Experiments in Fluids*, vol. 32, pp. 294-301, 2002.
- [4] F. Aloui and S. Madani, "Experimental investigation of a wet foam flow through a horizontal sudden expansion", *Experimental Thermal and Fluid Science*, vol. 32, pp. 905-926, 2008.
- [5] F. Aloui and S. Madani, "Wet foam flow under a fence located in the middle of a horizontal duct of square section" *Colloid. and Surface. A*, vol. 309, pp. 71-86, 2007.
- [6] P. Tisné, L. Doublier, and F. Aloui, "Determination of the slip layer thickness for a wet foam flow" *Colloids Surf. A: Physicochem. Eng. Aspects*, vol. 246, pp. 21-29, 2004.

- [7] Z.X. Mao and Hanratty T.J., "The use of scalar transport probes to measure wall shear stress in a flow with imposed oscillations" *Expt. Fluids*, vol. 3, p. 129, 1985.
- [8] R. Chovet and F. Aloui, "Gas-liquid foam through a straight duct and singularities: CFD simulations and experiments", *Proceedings of the ASME 2014 FEDSM*, no. FEDSM2014-21190, August 2014.
- [9] R. Chovet, F. Aloui, and L. Labraga, "Wet foam flow in horizontal square ducts and through singularities", *Proceedings of the ASME 2013 FEDSM*, no. FEDSM2013-16307, July 2013.
- [10] M.A. Lévêque, "Les lois de la transmission de la chaleur par convection", *Ann. Mines Carbur.*, vol. 13, pp. 201-239, 1928.
- [11] P. Tisné, "Etude par la méthode polarographique des contraintes pariétales exercées par une mousse en écoulement", Nantes, France, PhD. Thesis, 2003.
- [12] N.D. Denkov, S.S. Tcholakova, R Höhler, and S. Cohen-Addad, "Foam Rheology" in *Foam Engineering: Fundamentals and Applications*, John Wiley & Sons, 2012, pp. 91-120.
- [13] J. Plateau, "5th and 6th Series" *Mem. Acad. Roy. Sci. Belg.*, vol. 33, 1861.
- [14] D. Weaire, "The rheology of foam", *Progress in Colloid and Polymer Science*, vol. 133, pp. 100-105, 2006.